

EgoCross: Benchmarking Multimodal Large Language Models for Cross-Domain Egocentric Video Question Answering

Yanjun Li^{1*}, Yuqian Fu^{2*}, Tianwen Qian^{1†}, Qi’ao Xu¹, Silong Dai¹,
Danda Pani Paudel², Luc Van Gool², Xiaoling Wang^{1†}

¹School of Computer Science and Technology, East China Normal University

²INSAIT, Sofia University “St. Kliment Ohridski”

Abstract

Recent advances in Multimodal Large Language Models (MLLMs) have significantly pushed the frontier of egocentric video question answering (EgocentricQA). However, existing benchmarks and studies are mainly limited to common daily activities such as cooking and cleaning. In contrast, real-world deployment inevitably encounters domain shifts, where target domains differ substantially in both visual style and semantic content. To bridge this gap, we introduce **EgoCross**, a comprehensive benchmark designed to evaluate the cross-domain generalization of MLLMs in EgocentricQA. EgoCross covers four diverse and challenging domains, including surgery, industry, extreme sports, and animal perspective, representing realistic and high-impact application scenarios. It comprises approximately 1,000 QA pairs across 798 video clips, spanning four key QA tasks: prediction, recognition, localization, and counting. Each QA pair provides both OpenQA and CloseQA formats to support fine-grained evaluation. Extensive experiments show that most existing MLLMs, whether general-purpose or egocentric-specialized, struggle to generalize to domains beyond daily life, highlighting the limitations of current models. Furthermore, we conduct several pilot studies, e.g., fine-tuning and reinforcement learning, to explore potential improvements. We hope EgoCross and our accompanying analysis will serve as a foundation for advancing domain-adaptive, robust egocentric video understanding.

Code — <https://github.com/MyUniverse0726/EgoCross>

Challenge — <https://egocross-benchmark.github.io/>

1 Introduction

Egocentric videos, which capture how humans perceive and interact with the physical world from a first-person perspective, offer a rich and unique source of data for modeling human behaviors. Understanding egocentric vision is therefore highly valuable for applications such as embodied AI, wearable assistants, and human-to-robot learning. Among various egocentric tasks, video question answering (VQA) (Zhong et al. 2022) has emerged as a particularly challenging yet impactful problem. Early efforts

like EgoVQA (Fan 2019), EgoTaskQA (Jia et al. 2022), and EgoSchema (Mangalam, Akshulakov, and Malik 2023) laid the groundwork for EgocentricQA by introducing dedicated benchmarks. The rapid progress of Multimodal Large Language Models (MLLMs) has further significantly advanced this field in both benchmark construction and model development. On the benchmark side, EgoThink (Cheng et al. 2024), EgoTempo (Plizzari et al. 2025), and Ego-TextVQA (Zhou et al. 2025) have been proposed, targeting different aspects of the QA task. On the modeling side, a number of MLLMs specifically designed or adapted for egocentric video understanding have also emerged. Notable examples include EgoVLPv2 (Pramanick et al. 2023) and EgoGPT (Yang et al. 2025), which extend general-purpose MLLMs for EgocentricQA by training on specialized egocentric data.

Despite recent progress, most existing works remain focused on common daily-life activities, such as cooking, eating, and gardening. However, real-world applications inevitably extend beyond such scenarios. For example, in a surgical setting, a model must not only recognize a generic “cutting tool” but also precisely differentiate between instruments like a grasper, a cautery hook, and bipolar forceps. In such cases, both the visual appearance and the semantic context deviate significantly from those found in everyday activities. This naturally raises a fundamental question: *Can existing MLLMs generalize effectively to these uncommon and domain-specific scenarios?*

To answer this question, we introduce **EgoCross**, a comprehensive benchmark designed to evaluate the cross-domain generalization capabilities of MLLMs in EgocentricQA. EgoCross is built upon three core design principles: ① emphasis on cross-domain properties, ② relevance to practical applications, and ③ fine-grained, multi-dimensional model assessment. Following these principles, we carefully curated video sources and developed corresponding QA pairs to reflect real-world, high-impact use cases. Specifically, we selected surgery, industry, extreme sports, and animal perspective, as the four basic domains of our benchmark. These domains exhibit substantial visual and semantic deviations from typical daily-life scenarios, thus posing unique challenges for model generalization. Based on these video sources, we designed a structured data curation pipeline to construct QA pairs across

*These authors contributed equally.

†Corresponding authors.

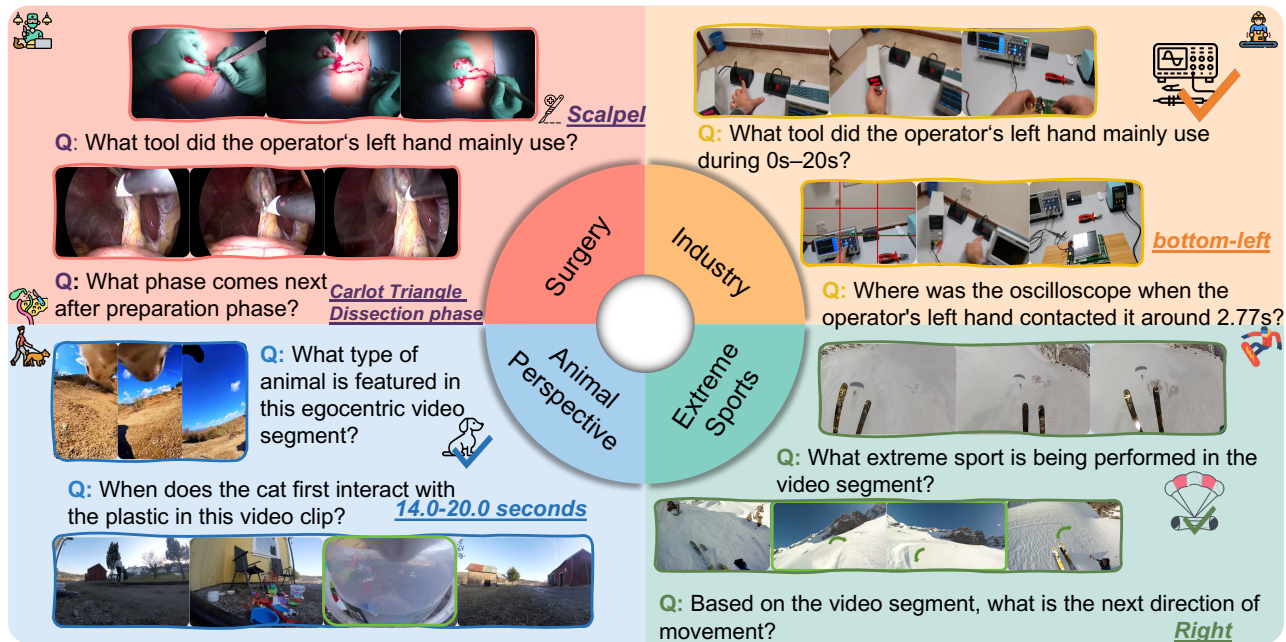


Figure 1: **Examples of Our EgoCross Benchmark.** We go beyond everyday egocentric scenarios, covering four diverse, cross-domain, application-oriented areas: Surgery, Industry, Extreme Sports, and Animal Perspective. As shown in the examples, both the visual appearances and the semantic content differ significantly from existing EgocentricQA datasets.

four fundamental QA task types: *identification*, *localization*, *prediction*, and *counting*, further spanning a total of 15 specific subtasks. To support both discriminative and generative evaluation protocols, each QA instance is annotated in both CloseQA (multiple-choice) and OpenQA (free-form answer) formats. In total, EgoCross consists of approximately 1,000 QA pairs across 798 egocentric video clips, forming a carefully constructed dataset that enables systematic evaluation of cross-domain generalization in EgocentricQA. A visual overview and representative examples are provided in Fig. 1.

Experiments demonstrate that most general-purpose and egocentric-specific MLLMs struggle on EgoCross, with CloseQA accuracy below 55% (random chance: 25%) and OpenQA below 35%, revealing their limitations in cross-domain settings. A notable performance drop ($1.6\times\downarrow$) on the same question types from EgoSchema to our EgoCross further confirms the challenge. We also explored prompt learning, fine-tuning, and reinforcement learning to assess potential improvements, offering insights for future research.

Our main contributions are summarized as follows:

- We are the first to define and motivate the task of cross-domain EgocentricQA, an underexplored yet crucial area for real-world application.
- We release EgoCross, the first cross-domain benchmark for EgocentricQA, covering four distinct domains (surgery, industry, extreme sports, and animal perspective) with $\sim 1k$ high-quality QA pairs.
- We conduct a comprehensive evaluation across 8 state-of-the-art MLLMs, quantitatively revealing their limitations beyond daily-life domains and highlighting the

need for more domain-robust models.

- We provide forward-looking pilot studies, offering actionable insights and shedding light on future directions for building more generalizable and robust MLLMs.

2 Related Work

2.1 Egocentric Video Understanding

Egocentric video understanding, modeling human perception from a first-person view, has gained growing attention. Beyond basic perception (Wang et al. 2021, 2023), EgocentricQA has emerged as a key task. Initial benchmarks like EgoVQA (Fan 2019), EgoTaskQA (Jia et al. 2022), and EgoSchema (Mangalam, Akshulakov, and Malik 2023) have been joined by new datasets focusing on complex reasoning (Cheng et al. 2024), temporal understanding (Plizzari et al. 2025), and scene text (Zhou et al. 2025). The increasing data has also spurred the development of specialized models for egocentric video understanding, typically adapted from MLLMs. However, most existing work remains confined to daily-life scenarios, with limited attention paid to domain shifts. Our work fills this gap by introducing the first cross-domain testbed for EgocentricQA, emphasizing real-world, out-of-distribution targets.

2.2 MLLMs for Video Understanding

Recent MLLMs have shown remarkable capabilities in video understanding. General MLLMs such as GPT-4.1 (Achiam et al. 2023), Gemini 2.5 Pro (Comanici et al. 2025), Qwen2.5-VL (Bai et al. 2025), and InternVL (Zhu et al. 2025) achieve strong performance across a range of

video tasks through extensive multimodal pretraining. In parallel, specialized models like Video-LLaMA3 (Zhang et al. 2025) further improve temporal reasoning via dedicated architectural designs. Several MLLMs have also been tailored specifically for egocentric video understanding, including EgoVLPv2 (Pramanick et al. 2023) and EgoGPT (Yang et al. 2025). While these models perform well on third-person videos and egocentric videos from common daily scenarios, their ability to generalize to unfamiliar, domain-specific scenarios remains largely unexamined. In this work, we systematically assess how well the current state-of-the-art MLLMs generalize to cross-domain egocentric targets, revealing their limitations and offering in-depth analysis to facilitate future research in this direction.

2.3 Cross-Domain Generalization

Cross-domain generalization is a broad and long-standing challenge in computer vision. Prior work has investigated it across various tasks, including image classification (Zhu, Zhuang, and Wang 2019; Fu et al. 2023; Zhao et al. 2020), object detection (Zheng et al. 2020; Li et al. 2025; Zhang et al. 2022), and action recognition (Pan et al. 2020; Xu et al. 2022; Chen et al. 2021a), often leveraging domain transfer, data augmentation, efficient fine-tuning, and meta-learning techniques (Chen et al. 2021b). However, these efforts have primarily focused on third-person viewpoints and low-level perception tasks. In egocentric video understanding, domain shifts are particularly pronounced due to drastic variations in scenes, task semantics, and camera motion. While some works explore cross-domain few-shot recognition in egocentric videos (Hatano et al. 2024) or leverage large models for few-shot knowledge transfer (Ge et al. 2023), these remain limited to low-level perception tasks or more general settings. In contrast, EgoCross is the first benchmark specifically designed to evaluate cross-domain generalization in EgocentricQA, tackling both domain gap and high-level reasoning challenges.

3 EgoCross Dataset

In this section, we provide a comprehensive introduction to the EgoCross benchmark. We begin by discussing the selection of domains, video sources, and the taxonomy of question-answering tasks, followed by an explanation of the data curation pipeline, and conclude with its dataset statistics.

3.1 Source Selection and Task Taxonomy

Design Principles. We established key principles for domain and dataset selection, as well as question-answering task taxonomy: ① *Emphasis on Cross-Domain Properties.* We need to select domains with distinct knowledge structures, terminologies, and interactions that differ significantly from everyday scenarios, ensuring the models are challenged by unfamiliar concepts. ② *Impact on Practical Applications.* Datasets closely related to real-world applications, e.g., healthcare and industrial operations, are encouraged, as they are expected to foster progress toward practical applications of EgocentricQA. ③ *Fine-grained Multi-dimensional*

Model Assessment. Tasks should span a broad range, covering diverse examination types, such as complex reasoning and spatiotemporal dependencies, and also with comprehensive evaluation metrics.

Domain and Data Source Selection. Based on the above criteria, we select four professional domains that present distinct challenges and high real-world relevance: *surgery*, *industry*, *extreme sports*, and *animal perspective*. For each, we curated one or two high-quality, open-source datasets with expert-provided meta annotations, each presenting unique perceptual, cognitive, and reasoning demands. The selected domains and the corresponding datasets are as follows:

- **Surgery.** The surgical domain represents a highly structured, knowledge-intensive scenario where precision, sequential understanding, and risk-awareness are paramount. To enrich visual diversity, we include two datasets: *EgoSurgery* (Fujii et al. 2024), which records the videos of open-heart surgeries from the surgeon’s perspective, with fine-grained annotations of hand-tool interactions and surgical phases; and *CholecTrack20* (Nwoye et al. 2025), which offers laparoscopic videos of cholecystectomy procedures from a tool-centered perspective. This dataset offers a rare yet insightful egocentric perspective captured from a tool rather than a typical human operator.
- **Industry.** Complex workflows in industrial scenarios demand not only perception of fine object manipulations but also reasoning over procedural sequences and tool-usage logic. We choose *ENIGMA-51* (Ragusa et al. 2024), a dataset containing real circuit board repair tasks.
- **Extreme Sports.** Extreme sports pose unique challenges, such as rare environments, rapid camera motion, and blur, which could well test models’ spatiotemporal perception and high-speed situational reasoning. We include the *ExtremeSportFPV* (Singh, Arora, and Jawahar 2017), which features first-person videos of various extreme sports, including mountain biking, skiing, and skydiving.
- **Animal Perspective.** To challenge anthropocentric bias in existing models, we introduce the animal perspective, introducing new motion patterns, camera angles, and semantic focus to the models. *EgoPet* (Bar et al. 2024), a dataset featuring egocentric views from animals such as dogs, cats, eagles, and turtles, is thus included.

The selected domains and video sources align well with our principles ① and ②.

QA Task Taxonomy. Following Principle ③, we aim to construct diverse QA pairs to comprehensively assess model capabilities. As illustrated in Fig. 3, our evaluation framework is built around four core task categories: *Identification*, *Localization*, *Prediction*, and *Counting*. Tailored to address the unique challenges of each domain, we further decompose these four broad categories into 15 specific sub-tasks, collectively forming a comprehensive evaluation framework. In the following, we provide an overview of the 4 core tasks. Detailed sub-tasks and representative examples can be found in Fig. 3 and Appendix.

- **Identification.** Identification tasks evaluate a model’s ability to recognize objects, actions, and events within a video. These tasks require domain-specific knowledge and adaptation to subtle differences in object properties or actions across contexts. For example, in surgical scenarios, instruments like forceps and scissors share similar shapes and colors, placing high demands on the models.
- **Localization.** Localization tasks assess a model’s ability to identify the precise spatial or temporal location of objects, actions, or interactions. These tasks require the model to understand spatiotemporal relationships and adjust to the variations in object positioning and motion patterns across different environments. In industrial assembly, for example, locating tools or components in a cluttered workspace is particularly challenging due to partial occlusions and rapid movements of small objects.
- **Prediction.** Prediction tasks test a model’s ability to forecast future actions or outcomes based on the current content. Thus, models are expected to grasp the underlying procedural or causal relationships in unseen domains. For example, in surgery, predicting the next phase of the procedure, such as transitioning from suturing to wound closure, relies on models’ understanding of established surgical patterns, which can vary significantly across different domains like industrial assembly or extreme sports.
- **Counting.** Counting tasks evaluate a model’s ability to track and count distinct instances or occurrences over time. These tasks require precise identification and temporal aggregation of visual elements, which becomes increasingly complex when dealing with fast-paced or dynamic scenarios. In extreme sports, for example, counting the number of tricks or jumps requires tracking high-velocity actions and differentiating between overlapping movements in a dynamic, cluttered environment.

3.2 Data Curation Pipeline

Based on the selected data sources and question categories, we developed a multi-stage curation pipeline (Fig. 2) with three key stages: meta annotation refinement, QA template design, and batch generation with quality control. The detailed procedures are described below.

Meta Annotation Refinement. Although the selected datasets provide original annotations, these are typically tailored for simpler, task-specific objectives such as 2D spatial bounding boxes for tool interactions or temporal segments for action classification. In addition, the annotation formats vary significantly between datasets. To address this, we performed a comprehensive refinement process that involved unifying annotation formats and conducting manual reviews to ensure the label accuracy. This refinement step was essential for constructing a reliable ground truth, which serves as the foundation for all subsequent QA generation.

QA Template Design. Following the task taxonomy, we manually designed 8 initial QA templates by creating two for each of the four core task categories. To enhance linguistic diversity and complexity, we employed a large language model (Gemini 2.5 pro) to expand the initial templates

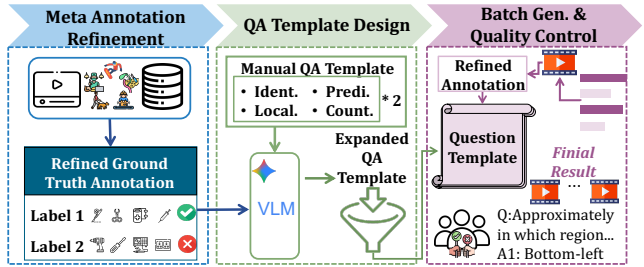


Figure 2: Data construction pipeline of EgoCross.

by generating domain-specific sub-tasks, using the original templates and refined annotations. All LLM-generated questions were then rigorously verified by human annotators to ensure clarity, logical consistency, and answerability based on the video content. Annotators also specified the programmatic reasoning steps and the expected answer format (e.g., object names, timestamps) for each template to ensure that the questions are both challenging and solvable.

Batch Generation and Final Quality Control. After obtaining the question templates, we perform batch instantiation to generate final QA pairs. For each sampled template, we first randomly extract a corresponding video clips based on its predefined duration, and then derive the ground-truth answer by executing the associated programmatic reasoning over the cropped clips. For comprehensive evaluation, we adopt both the traditional closed-form multiple-choice format (CloseQA) and a more flexible open-ended format (OpenQA) for the answers. In CloseQA, each question is accompanied by one correct answer and three distractors randomly sampled from the same answer type. For OpenQA, the answer consists of the full reasoning steps, which is further refined by a LLM. To ensure the data quality at scale, we conducted a final quality control check by randomly sampling and verifying 10% of QA pairs from each domain.

3.3 Dataset Statistics

Our EgoCross benchmark covers four diverse domains: Surgery, Industry, Extreme Sports (XSports), and Animal Perspective (Animal Per.), sourced from five real-world ego-centric video datasets. It comprises 798 video clips and 957 QA pairs, spanning 15 sub-task types grouped into four main categories. Tab.1 summarizes key statistics of the five datasets, including the number of clips, QA pairs, and average seconds of video durations (Dur.(s)). Fig.3 further illustrates the composition of EgoCross, including: the distribution of the four primary QA task categories, the 15 sub-task types, the question counts across domains, and representative QA examples for each major capability.

4 Experiments

4.1 Experimental Setup

Evaluated Models. We select a diverse set of MLLMs spanning three categories to cover major technical

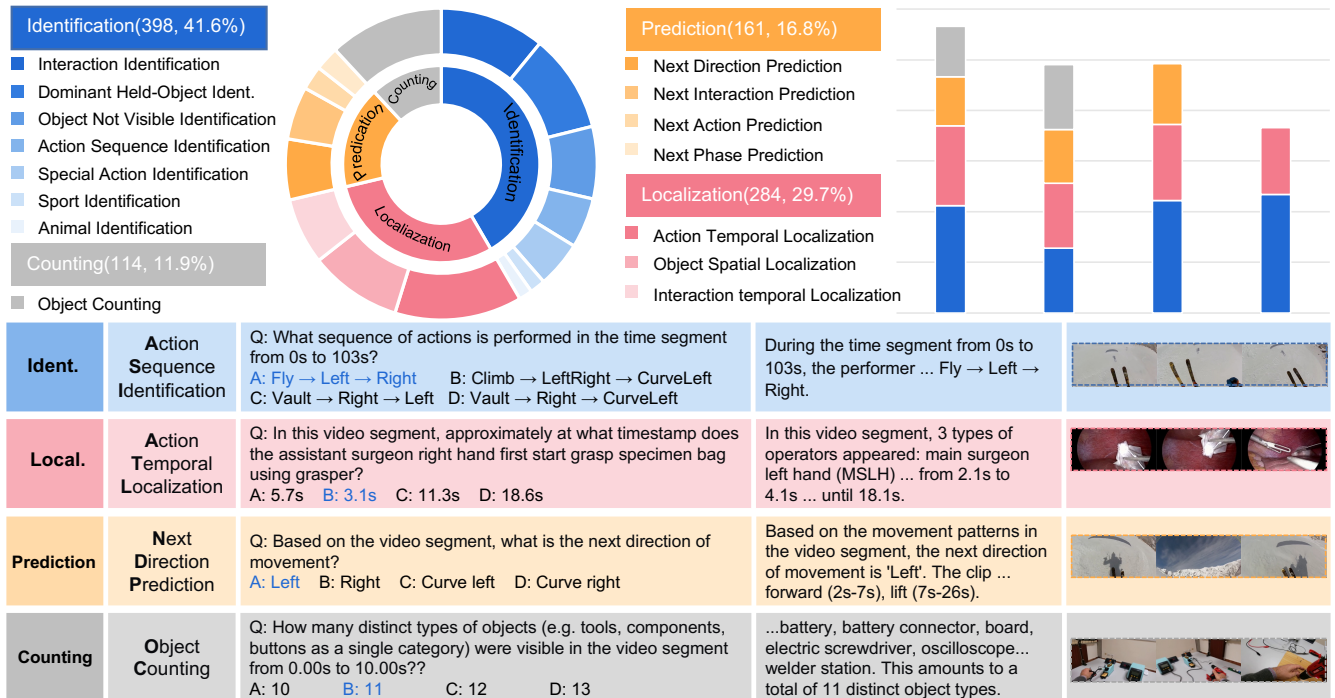


Figure 3: An overview of the EgoCross task taxonomy and statistics. (Top-left) The overall distribution of the four main task categories: Identification, Localization, Prediction, and Counting. (Top-right) The number of questions across the four primary domains. (Bottom) A selection of representative QA examples for each major capability is presented. For a more comprehensive list of examples, please see the Appendix.

Domain	Source	Clips	QA Pairs	Dur.(s)
Surgery	CholecTrack20	112	183	29.7
	EgoSurgery	100	100	20.4
Industry	ENIGMA-51	176	245	16.5
XSports	ExtremeSportFPV	242	246	13.7
Animal Per.	EgoPet	168	183	31.5
EgoCross	5 datasets	798	957	22.5

Table 1: Key statistics of EgoCross benchmark.

paradigms: 1) To assess the current state-of-the-art performance, we include leading proprietary models: GPT-4.1 (Achiam et al. 2023) and Gemini 2.5 Pro (Comanici et al. 2025). 2) For open-source general-purpose MLLMs, we consider Qwen2.5-VL (3B, 7B) (Bai et al. 2025), VideoLLaMA3 (Zhang et al. 2025), and InternVL3 (Zhu et al. 2025). 3) To evaluate models tailored for egocentric understanding, we also include two egocentric-specialized models: EgoVLPv2 (Pramanick et al. 2023), and EgoGPT (Yang et al. 2025).

Evaluation Metrics. Following prior works (Fan 2019; Mangalam, Akshulakov, and Malik 2023; Plizzari et al. 2025), we use standard *accuracy* metric for CloseQA, which is calculated as the percentage of correctly answered questions. For OpenQA, we employ a two-stage evaluation pro-

cess: 1) a direct exact match between the generated and ground-truth answer, and 2) if no match is found, we adopt a *LLM-as-a-Judge* approach to evaluate semantic correctness. Specifically, Qwen-MAX serves as the judge, providing a binary judgment (Correct/Incorrect) along with a detailed rationale for its decision. This ensures a robust assessment of semantic equivalence beyond simple string matching.

Implementation Details. All MLLMs are tested in a zero-shot setting with single-round inference. For video input, we extract frames at a fixed rate of 0.5 fps. For datasets that provide pre-sampled frames, we adhere to their original sampling frequency (e.g., EgoSurgery at 0.5 fps and parts of CholecTrack20 at 1 fps). No maximum frame limit is imposed to allow models to process the full temporal context. All experiments are conducted on NVIDIA A6000 GPUs. More implementation details can be found in the Appendix.

4.2 Results on EgoCross

Evaluation results are summarized in Tab. 2. We analyze the outcomes from four perspectives: 1) task-level challenges, 2) inter-domain variance, 3) model-wise performance, and 4) metric-type analysis.

Task-level Challenges. Most evaluated MLLMs struggle to perform well on our EgoCross benchmark, with average scores falling below 55% on CloseQA and below 35% on OpenQA. Considering that the random guess accuracy

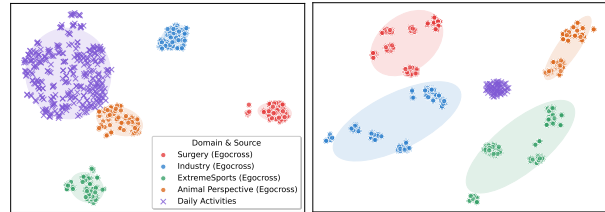
Models	Surgery		Industry		XSports		Animal Per.		Overall	
	Closed	Open								
<i>Proprietary MLLMs</i>										
GPT-4.1	<u>57.24</u>	<u>39.58</u>	45.71	12.24	<u>43.09</u>	<u>20.33</u>	<u>64.48</u>	<u>34.43</u>	<u>52.63</u>	<u>26.65</u>
Gemini 2.5 Pro	61.48	42.40	37.55	24.49	43.90	21.54	68.85	49.18	52.95	34.40
<i>Open-source MLLMs</i>										
Qwen2.5-VL-3B	35.69	16.96	36.33	6.94	36.59	6.91	41.53	28.42	37.54	14.81
Qwen2.5-VL-7B	46.29	21.55	37.55	<u>22.04</u>	41.87	6.91	53.55	31.15	44.82	20.41
VideoLLaMA3-7B	39.22	15.90	<u>40.82</u>	13.47	37.80	13.41	50.27	32.24	42.03	18.76
InternVL3-8B	47.00	17.67	33.06	11.84	41.06	11.38	49.18	30.60	42.58	17.87
<i>Egocentric MLLMs</i>										
EgoVLPv2	26.50	-	34.69	-	23.17	-	24.04	-	27.10	-
EgoGPT	31.80	13.07	24.49	10.20	24.80	13.82	41.53	26.78	30.66	15.97

Table 2: Evaluation results of MLLMs on EgoCross. All scores are reported in percentages. The best results are marked in **bold**, and the second-best are underlined. EgoVLPv2 is not evaluated on open-set tasks due to its model architecture.

for CloseQA is 25%, these results suggest that the models indeed face substantial challenges in this benchmark. Furthermore, excluding the top performance from proprietary models (Gemini 2.5 Pro and GPT-4.1), the remaining models perform notably worse, achieving less than 45% on CloseQA and under 20% on OpenQA. These observations collectively underscore both the difficulty and value of the proposed EgoCross benchmark, while also highlighting the current limitations of state-of-the-art MLLMs in handling cross-domain tasks.

Inter-Domain Variance. Across target domains, we observe varying levels of difficulty, ranging from relatively easy (Animal Perspective), middle-hard (Surgery) to particularly challenging (Extreme Sports, Industry). To further investigate inter-domain variance, we visualize t-SNE embeddings of EgoSchema and the four out-of-domain targets, using CLIP (Radford et al. 2021) as a modality-aligned feature extractor for both visual and textual representations (Fig. 4). The analysis highlights three key findings: 1) All target domains are clearly separated from EgoSchema and from each other in both visual and textual spaces, confirming the dataset’s cross-domain and diverse nature. 2) Within each of our target domains, textual features form sub-clusters, indicating the richness of our QA pairs. 3) The distributions help explain domain difficulty: Animal Perspective is closest to EgoSchema in both modalities, aligning with its relatively easier performance. In contrast, Industry and Extreme Sports are farthest, consistent with their higher difficulty. Surgery seems as a visual outlier but achieves relatively strong performance, suggesting that advanced MLLMs may be more robust to perceptual variation while still challenged by deeper semantic reasoning.

Model-wise Performance. As briefly discussed above, the two proprietary MLLMs achieve the highest overall performance, with Gemini 2.5 Pro outperforming GPT-4.1. This superiority is expected, given their access to large-scale training data and advanced algorithmic design. Following them are the open-source models, including Qwen2.5-



(a) Visual features t-SNE. (b) Text features t-SNE.

Figure 4: t-SNE visualization of text and visual features. EgoCross domains are color-coded: Surgery (red), Industry (blue), ExtremeSports (green), Animal Perspective (orange) and Daily-activity (purple).

VL, VideoLLaMA3, and InternVL3. Compared to proprietary models, they exhibit clear performance drops on both CloseQA and OpenQA tasks, highlighting the substantial gap that remains in tackling cross-domain egocentric understanding within the open-source community. Surprisingly, the egocentric-specific models (EgoVLPv2, and EgoGPT) perform the worst, despite being explicitly designed and trained on egocentric video data. Their failure, in contrast to general-purpose models, more clearly underscores the challenge of cross-domain generalization.

Metric-type Analysis. We further analyze the results under different evaluation metrics, namely CloseQA and OpenQA. Since CloseQA simplifies the task by providing explicit candidate answers, models naturally achieve higher accuracy in CloseQA compared to OpenQA. Additionally, we observe that CloseQA scores tend to be more stable across different MLLMs, while OpenQA is more sensitive to variations. For example, GPT-4.1 and Gemini 2.5 Pro achieve nearly identical scores on CloseQA (52.63 vs. 52.95), but differ noticeably on OpenQA (26.65 vs. 34.40). These observations confirm that OpenQA presents a more challenging setting, reflecting a common limitation of current MLLMs: their generative abilities are generally weaker than their judgment ca-

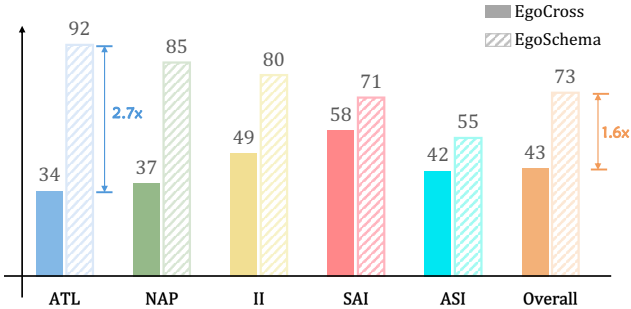


Figure 5: In-domain and cross-domain accuracy comparison across five QA types: Action Temporal Localization (ATL); Next Action Prediction (NAP); Interaction Identification (II); Special Action Identification (SAI); Action Sequence Identification (ASI). The results highlight the performance gap when evaluating on novel domains.

pabilities. By evaluating both OpenQA and CloseQA, we aim to comprehensively assess the generative and judgmental capacities of MLLMs in cross-domain scenarios.

In addition to dataset-level experiments and analysis, we conduct a more fine-grained evaluation across different QA types. Due to space limitations, detailed results and discussions are provided in the Appendix.

4.3 More Analysis on Cross-Domain Gap

In Sec. 4.2, we demonstrate that domain gaps significantly contribute to the overall low performance. To further investigate this effect and highlight its unique presence in EgoCross, we compare model performance between our benchmark and EgoSchema (Mangalam, Akshulakov, and Malik 2023), a typical daily-life egocentric dataset featuring common activities like cooking and cleaning. To ensure a comparison across analogous QA types, we devise a semi-automated QA type categorization process to align EgoSchema’s QA pairs with our tasks. The detailed procedure is provided in the Appendix. Based on these aligned QA pairs, we evaluate Qwen2.5-VL, which achieves the best results among open-source MLLMs, on tasks from both EgoSchema (in-domain) and EgoCross (cross-domain) using the CloseQA protocol.

Results in Fig. 5 reveal a consistent and significant performance drop across all comparable QA types. For instance, performance on *action temporal localization* drops from an impressive 92.31% on in-domain EgoSchema to just 34.13% on the novel domains of surgery, industry, and extreme sports in EgoCross. Similarly, *next action prediction* accuracy falls from 85.71% to 37.50%. The overall accuracy also drops from 73.58% to 43.14%, quantifying the substantial penalty incurred by the domain shift. This task-level analysis reinforces our core finding: despite strong results on existing egocentric benchmarks, current MLLMs lack robustness when applied to unseen, domain-specific settings, a limitation largely overlooked in prior work.

Method	Surgery	Industry	XSports	Animal Per.	Avg.
Baseline*	46.29	37.55	41.87	53.55	44.82
Baseline	37.35	35.71	34.72	43.40	37.80
+Prompt	44.58	34.29	52.78	43.40	43.76
+SFT	37.35	52.86	40.28	43.40	43.47
+RL	49.40	61.43	54.17	75.47	60.12

Table 3: CloseQA accuracy in pilot studies. “+SFT” and “+RL” denote supervised fine-tuning and reinforcement learning, respectively. * denotes the baseline without vLLM acceleration, it is marked in gray as vLLM acceleration causes slight performance degradation.

4.4 Pilot Studies

We proactively conduct several pilot studies to explore potential solutions for improving cross-domain egocentric QA. Specifically, we investigate three techniques: prompt learning, supervised fine-tuning (SFT), and reinforcement learning (RL). Since both SFT and RL require labeled data, we randomly split the initial test QA pairs into training and testing sets with a 70%:30% ratio. We adopt Qwen2.5-VL-7B as the baseline, and apply vLLM (Kwon et al. 2023) for model acceleration. CloseQA results are shown in Tab. 3.

The results provide several insights: 1) *Overall Trend*. Each method, whether prompting (without labeled data) or SFT/RL (requiring labeled data), improves performance to some extent. This suggests that refining prompt designs, expanding labeled data, and advancing algorithms are all promising directions for future exploration. 2) *Impact of SFT*. SFT boosts accuracy in domains like Industry (nearly 20% improvement). However, in some domains, such as Animal Per. no improvement is observed. This may stem from the inherently higher base performance in this domain, which is closer to natural domains. It could be caused by the limited number of training samples (Animal Per. has only 128 samples, far fewer than other domains.), which restricts the effectiveness of SFT. 3) *Effectiveness of RL*. RL shows the most significant improvement across all domains (an average increase of 22%). We attribute this to RL’s ability to learn from a broader range of interactions and feedback during training. The trial-and-error process enables the model to better handle longer sequences and more complex decision-making tasks, allowing it to dynamically adapt to the unique challenges of each domain.

5 Conclusion

In this work, we present EgoCross, a new benchmark for evaluating the cross-domain generalization ability of Multimodal Large Language Models (MLLMs) in egocentric video question answering. EgoCross comprises approximately 1k QA pairs based on video clips carefully collected and curated from four diverse and realistic domains: surgery, industry, extreme sports, and animal perspective, supporting both CloseQA and OpenQA for fine-grained evaluation. Our extensive evaluation reveals that current SOTA MLLMs struggle to generalize to these unfamiliar domains, despite strong performance on existing benchmarks. Additionally, we further explore several potential techniques to improve

cross-domain generalization. We believe that EgoCross, together with our experiments and analysis, offers a valuable foundation for future research.

Acknowledgments

This work was supported by NSFC grant (No. 62136002 and 62477014), Ministry of Education Research Joint Fund Project (8091B042239), and Fundamental Research Funds for the Central Universities. Project supported by Shanghai Municipal Science and Technology Major Project (2025SHZDZX025G16).

References

- Achiam, J.; Adler, S.; Agarwal, S.; Ahmad, L.; Akkaya, I.; Aleman, F. L.; Almeida, D.; Altenschmidt, J.; Altman, S.; Anadkat, S.; et al. 2023. Gpt-4 technical report. *arXiv preprint arXiv:2303.08774*.
- Bai, S.; Chen, K.; Liu, X.; Wang, J.; Ge, W.; Song, S.; Dang, K.; Wang, P.; Wang, S.; Tang, J.; et al. 2025. Qwen2. 5-vl technical report. *arXiv preprint arXiv:2502.13923*.
- Bar, A.; Bakhtiar, A.; Tran, D.; Loquercio, A.; Rajasegaran, J.; LeCun, Y.; Globerson, A.; and Darrell, T. 2024. Egopet: Egomotion and interaction data from an animal’s perspective. In *European Conference on Computer Vision*.
- Chen, H.-P.; Le, T.-A.; Nguyen, T.-D.; D-Phuc, N.; Tran, M.-H.; Tran, T.-A.; Ho, T.-B.; Nguyen, A.-T.; and Nguyen, V.-K. 2021a. M3Net: Multi-view Encoding, Matching, and Fusion for Few-shot Fine-grained Action Recognition. In *Proceedings of the IEEE/CVF International Conference on Computer Vision Workshops*.
- Chen, Y.; Li, R.-J.; Wang, S.-Q.; Zhang, B.-J.; Zhang, C.; and Liu, C.-L. 2021b. Blockmix: Meta regularization and self-calibrated inference for metric-based meta-learning. In *Proceedings of the 35th AAAI Conference on Artificial Intelligence*, volume 35, 6779–6787.
- Cheng, S.; Guo, Z.; Wu, J.; Fang, K.; Li, P.; Liu, H.; and Liu, Y. 2024. Egothink: Evaluating first-person perspective thinking capability of vision-language models. In *Proceedings of the IEEE/CVF Conference on Computer Vision and Pattern Recognition*.
- Comanici, G.; Bieber, E.; Schaekermann, M.; Pasupat, I.; Sachdeva, N.; Dhillon, I.; Blistein, M.; Ram, O.; Zhang, D.; Rosen, E.; et al. 2025. Gemini 2.5: Pushing the frontier with advanced reasoning, multimodality, long context, and next generation agentic capabilities. *arXiv preprint arXiv:2507.06261*.
- Fan, C. 2019. Egovqa-an egocentric video question answering benchmark dataset. In *Proceedings of the IEEE/CVF International Conference on Computer Vision Workshops*.
- Fu, Y.; Xie, Y.; Fu, Y.; and Jiang, Y.-G. 2023. Styleadv: Meta style adversarial training for cross-domain few-shot learning. In *Proceedings of the IEEE/CVF conference on computer vision and pattern recognition*.
- Fujii, R.; Hatano, M.; Saito, H.; and Kajita, H. 2024. Egosurgery-phase: a dataset of surgical phase recognition from egocentric open surgery videos. In *International Conference on Medical Image Computing and Computer-Assisted Intervention*.
- Ge, Y.; Liu, Z.; Li, J.; Wang, Z.; Liu, Z.; Wu, G.; Wang, Y.; Zhu, Y.; Jin, G.; Yin, F.; and Tao, D. 2023. Connecting giants: Synergistic knowledge transfer of large multimodal models for few-shot learning. In *Advances in Neural Information Processing Systems*, volume 36.
- Hatano, M.; Hachiuma, R.; Fujii, R.; and Saito, H. 2024. Multimodal cross-domain few-shot learning for egocentric action recognition. In *European Conference on Computer Vision*.
- Jia, B.; Lei, T.; Zhu, S.-C.; and Huang, S. 2022. Egotaskqa: Understanding human tasks in egocentric videos. *Advances in Neural Information Processing Systems*.
- Kwon, W.; Li, Z.; Zhuang, S.; Sheng, Y.; Zheng, L.; Yu, C. H.; Gonzalez, J. E.; Zhang, H.; and Stoica, I. 2023. Efficient Memory Management for Large Language Model Serving with PagedAttention. In *Proceedings of the ACM SIGOPS 29th Symposium on Operating Systems Principles*.
- Li, Y.; Qiu, X.; Fu, Y.; Chen, J.; Qian, T.; Zheng, X.; Paudel, D. P.; Fu, Y.; Huang, X.; Van Gool, L.; et al. 2025. Domain-RAG: Retrieval-Guided Compositional Image Generation for Cross-Domain Few-Shot Object Detection. *arXiv preprint arXiv:2506.05872*.
- Mangalam, K.; Akshulakov, R.; and Malik, J. 2023. Egoschema: A diagnostic benchmark for very long-form video language understanding. *Advances in Neural Information Processing Systems*.
- Nwoye, C. I.; Elgohary, K.; Srinivas, A.; Zaid, F.; Lavanchy, J. L.; and Padoy, N. 2025. CholecTrack20: A Multi-Perspective Tracking Dataset for Surgical Tools. In *Proceedings of the IEEE/CVF Conference on Computer Vision and Pattern Recognition (CVPR)*.
- Pan, B.; Cao, Z.; Adeli, E.; and Niebles, J. C. 2020. Adversarial cross-domain action recognition with co-attention. In *Proceedings of the AAAI conference on artificial intelligence*.
- Plizzari, C.; Tonioni, A.; Xian, Y.; Kulshrestha, A.; and Tombari, F. 2025. Omnia de egotempo: Benchmarking temporal understanding of multi-modal llms in egocentric videos. In *Proceedings of the Computer Vision and Pattern Recognition Conference*.
- Pramanick, S.; Song, Y.; Nag, S.; Lin, K. Q.; Shah, H.; Shou, M. Z.; Chellappa, R.; and Zhang, P. 2023. Egovlpv2: Egocentric video-language pre-training with fusion in the backbone. In *Proceedings of the IEEE/CVF International Conference on Computer Vision*.
- Radford, A.; Kim, J. W.; Hallacy, C.; Ramesh, A.; Goh, G.; Agarwal, S.; Sastry, G.; Askell, A.; Mishkin, P.; Clark, J.; et al. 2021. Learning transferable visual models from natural language supervision. In *International conference on machine learning*.
- Ragusa, F.; Leonardi, R.; Mazzamuto, M.; Bonanno, C.; Scavo, R.; Furnari, A.; and Farinella, G. M. 2024. ENIGMA-51: Towards a Fine-Grained Understanding of Human Behavior in Industrial Scenarios. In *Proceedings of*

the *IEEE/CVF Winter Conference on Applications of Computer Vision*.

Singh, S.; Arora, C.; and Jawahar, C. 2017. Trajectory aligned features for first person action recognition. *Pattern Recognition*.

Wang, J.; Luvizon, D.; Xu, W.; Liu, L.; Sarkar, K.; and Theobalt, C. 2023. Scene-aware egocentric 3d human pose estimation. In *Proceedings of the IEEE/CVF Conference on Computer Vision and Pattern Recognition*.

Wang, X.; Zhu, L.; Wang, H.; and Yang, Y. 2021. Interactive prototype learning for egocentric action recognition. In *Proceedings of the IEEE/CVF International Conference on Computer Vision*.

Xu, Y.; Cao, H.; Mao, K.; Chen, Z.; Xie, L.; and Yang, J. 2022. Aligning correlation information for domain adaptation in action recognition. *IEEE Transactions on Neural Networks and Learning Systems*.

Yang, J.; Liu, S.; Guo, H.; Dong, Y.; Zhang, X.; Zhang, S.; Wang, P.; Zhou, Z.; Xie, B.; Wang, Z.; et al. 2025. Ego-life: Towards egocentric life assistant. In *Proceedings of the Computer Vision and Pattern Recognition Conference*.

Zhang, B.; Li, K.; Cheng, Z.; Hu, Z.; Yuan, Y.; Chen, G.; Leng, S.; Jiang, Y.; Zhang, H.; Li, X.; et al. 2025. VideoLLaMA 3: Frontier Multimodal Foundation Models for Image and Video Understanding. *arXiv preprint arXiv:2501.13106*.

Zhang, C.-B.; Li, G.-X.; Liu, H.-B.; Zhang, Y.-P.; and Li, X. 2022. Divide-and-conquer: Confluent triple-flow network for RGB-T salient object detection. *IEEE Transactions on Circuits and Systems for Video Technology*, 33(5): 2356–2368.

Zhao, J.-M.; Zhang, R.-Y.; Jia, Y.-J.; Zhang, Y.-W.; and Zhang, Q. 2020. Learning attention-guided pyramidal features for few-shot fine-grained recognition. In *Proceedings of the 28th ACM International Conference on Multimedia*, 1886–1894.

Zheng, Y.; Huang, D.; Liu, S.; and Wang, Y. 2020. Cross-domain object detection through coarse-to-fine feature adaptation. In *Proceedings of the IEEE/CVF conference on computer vision and pattern recognition*.

Zhong, Y.; Xiao, J.; Ji, W.; Li, Y.; Deng, W.; and Chua, T.-S. 2022. Video question answering: Datasets, algorithms and challenges. *arXiv preprint arXiv:2203.01225*.

Zhou, S.; Xiao, J.; Li, Q.; Li, Y.; Yang, X.; Guo, D.; Wang, M.; Chua, T.-S.; and Yao, A. 2025. Egotextvqa: Towards egocentric scene-text aware video question answering. In *Proceedings of the Computer Vision and Pattern Recognition Conference*.

Zhu, J.; Wang, W.; Chen, Z.; Liu, Z.; Ye, S.; Gu, L.; Tian, H.; Duan, Y.; Su, W.; Shao, J.; et al. 2025. InternV13: Exploring advanced training and test-time recipes for open-source multimodal models. *arXiv preprint arXiv:2504.10479*.

Zhu, Y.; Zhuang, F.; and Wang, D. 2019. Aligning domain-specific distribution and classifier for cross-domain classification from multiple sources. In *Proceedings of the AAAI conference on artificial intelligence*.

EgoCross: Benchmarking Multimodal Large Language Models for Cross-Domain Egocentric Video Question Answering

Supplementary Material

A Comparison with Existing Benchmarks

As shown in Table 4, EgoCross sets itself apart from prior benchmarks by uniquely integrating cross-domain challenges, temporal tasks, and a dual Open/Closed-QA format to provide a more rigorous and comprehensive evaluation of model generalization in egocentric video understanding.

B More Implement Details

This section provides a more detailed description of our experimental setup to support reproducibility and enable fair comparisons.

B.1 Implement Details of Main Experiments

This section supplements the settings from Section 4.1 to ensure full reproducibility of results reported in Section 4.2 and a fair comparison across all models.

Our evaluation methodology is based on a zero-shot, single-round inference paradigm, executed on NVIDIA A6000 GPUs. As previously mentioned, video frames are sampled at dataset-specific rates (0.5-1 fps) with no maximum frame limit. To guarantee deterministic and reproducible outputs, we set the key inference parameter `do_sample=False` for greedy decoding across all experiments. The exact prompts used for each task are detailed below to ensure a fair and standardized evaluation.

Close-ended Question Answering (CloseQA). For multiple-choice questions, the prompt illustrated in Figure 6 instructs the model to return its answer and reasoning in a structured JSON format. The letter following the “prediction” is then extracted as the final answer.

```
CloseQA Inference Prompt

Please carefully read the question and its options, then select the most appropriate answer. Question: {question}{options_str}
The original FPS of the video is {original_video_fps}. This image set is obtained by sampling at {sampling_fps} fps.
Respond in JSON format with two fields: 'prediction' (the correct option letter: A, B, C, or D) and 'reason' (a brief explanation of your choice). Do not include any other content.

Example response:
{
  "prediction": "B",
  "reason": "Paris is the capital city of France."
}
```

Figure 6: Prompt of CloseQA Inference

Open-ended Question Answering (OpenQA). For free-form questions, the prompt illustrated in Figure 7 guides the model in generating a textual answer. The string after the “prediction” is used as the model response for evaluation.

OpenQA Inference Prompt

Please carefully read the question and the provided context, then provide a clear and concise answer based on your understanding. Question: {question}
The original FPS of the video is {original_video_fps}. This image set is obtained by sampling at {sampling_fps} fps.
Your answer should be reasoned and directly address the question. Respond in JSON format with two fields: 'prediction' (your answer as text) and 'reason' (a brief explanation of your reasoning). Do not include any other content.

Example response:

```
{
  "prediction": "The time duration of the video is 10 seconds.",
  "reason": "The total number of frames is 240 and the frame rate is 24 FPS, so 240 / 24 = 10 seconds."
}
```

Figure 7: Prompt of OpenQA Inference

Evaluation Protocol for OpenQA. Given the subjective nature of open-ended answers, we employ Qwen-Max as an automated judge to ensure a consistent and scalable evaluation. The LLM judge evaluates the semantic correctness of the model prediction against the ground truth ground truth based on the prompts as shown in Figure 8

OpenQA LLM-as-Judge Prompt

You are an intelligent chatbot designed for evaluating the correctness of AI assistant predictions for question-answer pairs. Your task is to compare the predicted answer with the ground-truth and determine if the predicted answer is correct or not. Here's how you can accomplish the task:

##INSTRUCTIONS:

- Focus on the factual accuracy and semantic equivalence of the predicted answer with the ground-truth.
 - Consider uncertain predictions, such as 'it is impossible to answer the question from the video', as incorrect, unless the ground truth answer also says that.
- Please evaluate the following video-based question-answer pair:

Question: {question}
Correct ground truth: {answer}
Detailed ground truth: {detailed_answer}
Predicted Answer: {pred}

Provide your evaluation as a correct/incorrect prediction along with the score where the score is an integer value between 0 (fully wrong) and 5 (fully correct). The middle score provides the percentage of correctness. Please generate the response in the form of a json object with the following fields:

```
{
  "mark": 4, # The score of the prediction
  "reason": "", # The reason for the score
}
```

Figure 8: Prompt of LLM-as-Judge

B.2 Implement Details of Domain Gap Experiments

As mentioned in Section 4.3, to enable a direct comparison between the performance on EgoSchema (in-domain) and EgoCross (cross-domain), it was necessary to align the QA pairs from EgoSchema with our predefined task categories. Since EgoSchema does not provide official task-type labels, we developed a semi-automated, iterative categoriza-

Dataset	Cross Domain	Video Length	# Test	# Categories	Temporal	QA Types
EgoVQA	✗	(25s, 100s)	250	3	✗	OpenQA
EgoTaskQA	✗	25s	8k	4	✗	OpenQA
EgoSchema	✗	3 min	500	-	✗	CloseQA
EgoThink	✗	-	750	12	✗	OpenQA
EgoTempo	✗	45s	500	10	✓	OpenQA
EgoCross	✓	22.5s	957	15	✓	CloseQA & OpenQA

Table 4: Overview of each dataset’s characteristics, including average video length, number of test examples, number of categories, number of scenes where videos are captured, and question types (OpenQA or CloseQA).

tion process. This section details the methodology, the classification rules, and the final distribution of the aligned QA pairs.

Methodology for Semi-Automated Categorization To align the questions in EgoSchema with our predefined task categories, we employed a semi-automated workflow. We prompted a large language model (LLM) to generate keywords for each template of task type in EgoCross. These keywords were extracted to capture the core concepts and characteristics of each task type, such as identification, localization, prediction, and counting. We then used these keyword sets to classify the questions in EgoSchema by matching them to the relevant keywords. For categories with a limited number of questions, we avoided further subdivision to prevent statistical instability.

Crucially, this initial classification was refined through a rigorous human-in-the-loop process. Human experts reviewed the automated results, analyzed the question and options of misclassified instances, and iteratively updated the keyword lists. This refinement cycle was repeated for five rounds until the categorization stabilized and achieved high accuracy, as confirmed by final manual validation. This methodology produced a refined and consistent set of questions fully aligned with our task definitions.

Classification Rules and Keywords The refinement process yielded a set of keywords and a hierarchy to resolve ambiguities.

Classification Hierarchy. A strict priority order was established for overlapping cases:

- 1) **Main Categories:** Prediction → Counting → Localization → Identification.
- 2) **Identification Subtypes:** Dominant Held Object → Action Sequence → Interaction → Special Action.

Final Keyword Sets. The final keyword sets and question distribution are detailed in Table 6. To handle questions unique to EgoSchema, we designated *Inference Prediction* (which is absent in EgoCross) and created *Action State Identification* as a catch-all category for general action identification queries. The remaining six sub-tasks with non-zero counts constitute the core set of aligned task types used for our direct cross-dataset performance comparison.

Quantitative Cross-Domain Comparison. The significant performance gap between the two domains, illustrated in Figure 5, is quantitatively detailed in Table 5. To measure this gap, we evaluated Qwen2.5-VL on both the full datasets and our carefully aligned subsets. On the aligned subset of questions, the model’s accuracy plummets from 73.58% on in-domain EgoSchema tasks to just 43.14% on their cross-domain EgoCross counterparts. Notably, this performance trend on the subset closely mirrors the model’s overall results on the full datasets (69.60% on EgoSchema vs. 44.31% on EgoCross), validating that our aligned subset serves as a reliable proxy for evaluating the domain gap. The table further breaks down this degradation across analogous task types, highlighting that the domain shift poses a significant and consistent challenge to models’ capabilities.

Question Type	In-Domain		Cross-Domain	
	Num.	Acc. (%)	Num.	Acc. (%)
Special Action Id.	56	71.43	46	58.70
Interaction Id.	50	80.00	104	49.04
Temporal Loc.	26	92.31	126	34.13
Action Sequence Id.	47	55.32	50	42.00
Next Action Pred.	14	85.71	24	37.50
Overall Above	193	73.58	350	43.14
Overall Dataset	500	69.60	957	44.31

Table 5: A direct comparison of Qwen2.5-VL’s performance on analogous task types between the in-domain EgoSchema benchmark and our cross-domain EgoCross Benchmark. This highlights the stark performance degradation when transitioning to novel domains, even on structurally similar tasks.

B.3 Implement Details Of Pilot Studies

General Setup. To ensure consistency and efficiency across experiments, we employ the vLLM framework (Kwon et al. 2023) for both training and inference with the Qwen2.5-VL-7B model. While vLLM significantly accelerates these processes, we note a slight performance trade-off as shown in Table 3, which is an acceptable compromise, particularly for the extensive sampling required in

Category	Sub-tasks	Count	Keywords
Prediction	Next Action Prediction	14	<i>what will happen, future action, next phase, next direction, prepare for, ready for</i>
	Inference Prediction	26	<i>taking into account, analyze, evaluate, compare, discuss, deduce, overall focus</i>
Counting	Object Counting	0	<i>how many, number of, count how, quantity, total number</i>
Localization	Action Temporal Localization	26	<i>at what time, when did start/end/occur, key moments when, before, after, during</i>
	Object Spatial Localization	0	<i>where is/are, in which region/location, where located</i>
Identification	Dominant Held-Object Identification	10	<i>primary/main tool, tool used, effectiveness tools, how tools contribute</i>
	Action Sequence Identification	47	<i>sequence of actions, from start to finish, key steps, main stages, overarching process</i>
	Interaction Identification	50	<i>interaction between, two characters, both characters, collaborate, relationship</i>
	Special Action Identification	56	<i>most significant/important/critical, key turning points, pivotal, vital steps</i>
	Sport/Animal/Not Visible Identification	0	<i>sport, game play, animal, pet, not visible/shown/present</i>
	Action State Identification	239	<i>primary objective/goal, describe, summarize, explain, infer, deduce, what is/was primary</i>

Table 6: Final Keyword Sets and Question Distribution for EgoSchema Task Categorization.

RL training. All experiments were conducted on a server equipped with 8 NVIDIA H100 GPUs. The training setups for SFT and RL are inspired by the Video-R1 project, and we plan to release our code for reproducibility. For video inputs during training, we sample between 4 to 16 frames; sequences longer than 16 frames are truncated to 16. The inference settings for the pilot studies are kept consistent with those used for the main results.

Prompt Learning. The prompt for this method consists of two parts. The first part provides domain-specific context and examples, while the second part poses the direct question about the input video. This structure, illustrated in Figure 9, aims to guide the model towards the specific characteristics of each domain before it attempts to answer the question.

Supervised Fine-tuning (SFT). We perform full-parameter SFT on the base model, updating all of its weights. The training utilizes 4 H100 GPUs, with a per-device batch size of 1 and 2 gradient accumulation steps, resulting in an effective batch size of 8. We set the learning rate to $1e-6$ and train for 12 epochs. To manage memory and accelerate training, we leverage a suite of optimizations including DeepSpeed ZeRO-2, BF16 mixed precision, gradient checkpointing, and Flash Attention 2. The data

format used for SFT is shown in Figure 10.

Reinforcement Learning (RL). Our RL approach, based on Generative Reward-based Policy Optimization (GRPO), trains the model from scratch without an SFT warm-up. The training is distributed across all 8 H100 GPUs. We use a learning rate of $1e-6$ with a cosine scheduler and train for 16 epochs. The optimization strategy is intensified with DeepSpeed ZeRO-3 to accommodate the RL process, alongside BF16, gradient checkpointing, and Flash Attention 2. Key RL-specific hyperparameters include a reward-shaping beta of 0.04 and generating 8 responses per prompt during training for policy updates. The prompt structure for RL is depicted in Figure 11.

C More Experiment Results

C.1 CloseQA and OpenQA evaluations

This section provides detailed results for both CloseQA and OpenQA evaluations, broken down by task capabilities across different domains. The results are presented in Table 7 and Table 8.

To dissect the sources of this performance degradation, Table 7 and Table 8 provide a fine-grained analysis of CloseQA and OpenQA capabilities, respectively. This detailed breakdown reveals that the generalization gap is not

```

Domain Prompt Learning
"{Question}\n"
"Please think about this question as if you were a human pondering deeply,"
"then give your final answer between the <answer> </answer> tags."
{DOMAIN_CONTEXTS}
Please provide only the single option letter (e.g., A, B, C, D, etc.) within the
<answer> </answer> tags.

Domain Prompt
DOMAIN_CONTEXTS = {
  'Surgery': {
    'context': "Surgical procedure analysis from first-person perspective.
    Key focus: Precise tool identification, surgical phases, hand-specific
    operations."},
  'Industry': {
    'context': "Technical repair/assembly tasks from first-person perspective.
    Key focus: Component identification, systematic workflows,
    troubleshooting."},
  'Extreme Sports': {
    'context': "High-speed extreme sports from first-person perspective.
    Key focus: Motion patterns, terrain navigation, handling motion blur."},
  'Animal Perspective': {
    'context': "Animal perspective videos with alternative movement patterns.
    Key focus: Species identification, behavioral patterns, scale differences."}
}

```

Figure 9: The two-part prompt used for domain-specific prompt learning. The first part (top) provides domain context, and the second part (bottom) presents the specific question.

```

SFT Learning Prompt
"{Question}\n"
"Please think about this question as if you were a human pondering deeply,"
"then give your final answer between the <answer> </answer> tags."
Please provide only the single option letter (e.g., A, B, C, D, etc.) within the
<answer> </answer> tags.

```

Figure 10: The data format for SFT. Each sample consists of a video and a conversation, where the model is trained to generate the assistant’s response based on the user’s query.

uniform across different skills. In both evaluation settings, the proprietary SOTA models demonstrate a clear superiority in tasks requiring complex reasoning. This is most evident in the OpenQA **Prediction (P)** capability (Table 8), where Gemini 2.5 Pro achieves a remarkable 62.50% on surgical prediction, a task where most other models score in the single digits. This highlights that advanced temporal and causal reasoning is a key differentiator. In contrast, the performance gap narrows for more direct perceptual tasks like **Counting (C)**, where several open-source models exhibit competitive performance. This detailed view also uncovers intriguing failure modes. For instance, in the Animal Perspectives-Localization task, Gemini 2.5 Pro achieves a high score of 42.42%, while GPT-4.1 unexpectedly scores zero. A qualitative review reveals that while Gemini correctly provides timestamps, GPT-4.1 defaults to referencing frame indices (e.g., "The cat first interacts with the plastic in the fourth image"), failing to follow the prompt’s explicit instruction to use the provided video FPS. This specific failure, not observed in other domains for the same model, suggests its instruction-following capability can be brittle and context-dependent. Ultimately, this granular analysis con-

```

RL Learning Prompt
DOMAIN_CONTEXTS = {
  'Surgery': {
    'context': "Surgical procedure analysis from first-person perspective.
    Key focus: Precise tool identification, surgical phases, hand-specific
    operations."},
  'Industry': {
    'context': "Technical repair/assembly tasks from first-person perspective.
    Key focus: Component identification, systematic workflows,
    troubleshooting."},
  'Extreme Sports': {
    'context': "High-speed extreme sports from first-person perspective.
    Key focus: Motion patterns, terrain navigation, handling motion blur."},
  'Animal Perspective': {
    'context': "Animal perspective videos with alternative movement patterns.
    Key focus: Species identification, behavioral patterns, scale differences."}
}

```

Figure 11: The prompt structure for RL training. The model generates a response, which is then evaluated by a reward model to provide feedback for policy optimization.

firms the primary bottleneck: the challenge lies less in basic perception and more in the robust application of high-level skills—such as temporal reasoning, knowledge integration, and consistent instruction-following—within novel, specialized contexts.

D More Details of Datasets

This appendix provides detailed illustrative examples for the 15 sub-tasks within our proposed QA task taxonomy. As mentioned in the main text, these tasks are grouped into four core categories: **Identification, Localization, Prediction, and Counting**. Figure 12 showcases a representative question, closed answer, open answer and three corresponding visual frames for each sub-task, highlighting the diverse challenges across different egocentric video domains.

These examples cover scenarios ranging from fine-grained object recognition in surgical footage to high-level action anticipation in dynamic outdoor scenes, reflecting the breadth of reasoning skills required. Each sub-task is carefully crafted to target specific dimensions of egocentric understanding, such as detecting subtle hand-object interactions and predicting forthcoming activities from partial observations. Collectively, they constitute a rigorous and comprehensive benchmark for assessing multimodal models in realistic egocentric settings, where successful performance depends on the seamless integration of temporal context, visual detail, and task knowledge.

In the following, we present representative QA examples for all sub-tasks across four distinct domains — **Surgery** (Figure 13), **Industry** (Figure 14), **Extreme Sports** (Figure 15), and **Animal Perspective** (Figure 16).

Models	Surgery				Industry				XSports			Animal Per.	
	C	I	L	P	C	I	L	P	I	L	P	I	L
<i>Open-source MLLMs</i>													
Qwen2.5-VL-3B	34.00	44.34	30.38	27.08	29.69	<u>40.62</u>	34.38	41.51	53.15	25.33	20.00	47.01	31.82
Qwen2.5-VL-7B	<u>58.00</u>	50.00	<u>39.24</u>	37.50	29.69	37.50	45.31	37.74	52.25	29.33	38.33	52.99	54.55
InternVL3-8B	66.00	54.72	35.44	29.17	26.56	29.69	34.38	<u>43.40</u>	58.56	<u>28.00</u>	25.00	53.85	40.91
VideoLLaMA3-8B	34.00	46.23	<u>39.24</u>	29.17	<u>40.62</u>	<u>40.62</u>	26.56	58.49	52.25	<u>22.67</u>	<u>30.00</u>	60.68	31.82
<i>Egocentric MLLMs</i>													
EgoGPT	36.00	36.79	24.05	29.17	12.50	21.88	28.12	37.74	29.73	22.67	18.33	47.86	30.30
EgoVLPv2	20.00	33.02	26.58	18.75	45.31	29.69	31.25	32.08	21.62	24.00	25.00	25.64	21.21
<i>Proprietary MLLMs</i>													
GPT-4.1	54.00	<u>68.87</u>	35.44	<u>70.83</u>	34.38	54.69	<u>51.56</u>	41.51	66.67	26.67	20.00	79.49	37.88
Gemini 2.5 Pro	34.00	70.75	55.70	79.17	15.62	39.06	64.06	30.19	<u>63.06</u>	29.33	26.67	<u>78.63</u>	<u>51.52</u>

Table 7: Evaluation on Close-ended Questions. The task types are Counting (C), Identification (I), Localization (L), and Prediction (P). Best results are marked in **bold**, and the second-best is underlined.

Models	Surgery				Industry				Xsports			Animal Per.	
	C	I	L	P	C	I	L	P	I	L	P	I	L
<i>Open-source MLLMs</i>													
Qwen2.5-VL-3B	50.00	6.60	13.92	10.42	0.00	14.06	12.50	0.00	6.31	2.67	13.33	42.74	3.03
Qwen2.5-VL-7B	50.00	6.60	31.65	8.33	18.75	45.31	18.75	<u>1.89</u>	9.01	1.33	10.00	43.59	9.09
InternVL3-8B	40.00	15.09	12.66	8.33	1.56	<u>25.00</u>	18.75	0.00	8.11	12.00	16.67	45.30	4.55
VideoLLaMA3-8B	<u>46.00</u>	6.60	17.72	2.08	28.12	10.94	10.94	<u>1.89</u>	8.11	<u>21.33</u>	13.33	48.72	3.03
<i>Egocentric MLLMs</i>													
EgoGPT	38.00	4.72	13.92	4.17	4.69	12.50	<u>21.88</u>	0.00	6.31	<u>21.33</u>	18.33	41.88	0.00
<i>Proprietary MLLMs</i>													
GPT-4.1	<u>46.00</u>	31.13	40.51	<u>50.00</u>	9.38	18.75	15.62	3.77	21.62	6.67	35.00	53.85	0.00
Gemini 2.5 Pro	36.00	33.96	45.57	62.50	<u>26.56</u>	<u>25.00</u>	40.62	<u>1.89</u>	<u>17.12</u>	14.67	38.33	<u>52.99</u>	42.42

Table 8: Detailed evaluation on Open-ended Questions, broken down by capability type: Counting (C), Identification (I), Localization (L), and Prediction (P). All scores are in percentages. Best results are marked in **bold**, and the second-best is underlined.

Categories	Sub-tasks	Open-set Questions, Options and Answer	Close-set Answer	Video Frames
Identification	Interaction Identification	Q: What object is the cat interacting with in this video segment? A: Plastic B: Bench C: Vehicle D: Filament	The cat is interacting with a filament.	
	Dominant Held-Object Ident.	Q: Which tool was the operator's left hand predominantly interacting with in the video segment from 0.00s to 30.00s? A: Battery B: battery connector C: Board D: Button	During the segment from 0.00s to 21.01s, the operator's right hand ... with most frequently (10 instance(s)).	
	Object Not Visible Identification	Q: Which surgical instrument is NOT visible in the video segment from 0.00s to 60.00s? A: clipper B: irrigator C: scissors D: bipolar	In the segment, the following instruments are visible ... appear in this segment.	
	Action Sequence Identification	Q: What sequence of actions is performed in the time segment from 0s to 103s? A: Fly → Left → Right B: Climb → LeftRight → CurveLeft C: Vault → Right → Left D: Vault → Right → CurveLeft	During the time segment from 0s to 103s, the performer ... Fly → Left → Right.	
	Special Action Identification	Q: What action is being performed in the video segment from 6s to 8s? A: Spin B: Flip C: Jump D: Fly	The special action 'jump' is performed in the video ... a distinctive athletic maneuver.	
	Sport Identification	Q: What extreme sport is being performed in the video segment? A: Jetski B: Skiing C: Parkour D: Speedflying	The video shows skiing activity based on the movement patterns and environment.	
	Animal Identification	Q: What type of animal is featured in this egocentric video segment? A: Cheeatah B: Cat C: Turtle D: Alligator	The video shows a cat from an egocentric perspective.	
Localization	Action Temporal Localization	Q: In this video segment, approximately at what timestamp does the assistant surgeon right hand first start grasp specimen bag using grasper? A: 5.7s B: 3.1s C: 11.3s D: 18.6s	In this video segment, 3 types of operators appeared: main surgeon left hand (MSLH) ... from 2.1s to 4.1s ... until 18.1s.	
	Object Spatial Localization	Q: Approximately in which region of the view was the screwdriver located when the operator's right hand was in take with it around timestamp 3.33s? A: bottom-center B: bottom-left C: bottom-right D: center	An instance of interaction between the operator's right hand and the screwdriver...The screwdriver was determined to be in the 'bottom-right' region of the 3x3 grid overlay.	
	Interaction Temporal Local.	Q: When does the cat first interact with the plastic in this video clip? A: 13.4-15.4 seconds B: 10.1-12.1 seconds C: 2.2-4.2 seconds D: 6.5-8.5 seconds	The cat first interacts with the plastic from 6.0 to 9.0 seconds in this video clip.	
Prediction	Next Direction Prediction	Q: Based on the video segment, what is the next direction of movement? A: Left B: Right C: Curve left D: Curve right	Based on the movement patterns in the video segment, the next direction of movement is 'Left'. The clip ... forward (2s-7s), lift (7s-26s).	
	Next Interaction Prediction	Q: Based on the activity observed up to 30.00s, what is the predicted next type of interaction for the operator's left hand? A: contact the board B: contact the oscilloscope C: contact the oscilloscope component D: contact the pliers	At 2.47s, the right hand performed 'take' with 'board' ... at 25.87s approximately 1.07s. The predicted next interaction by the operator's left hand is 'contact the board'.	
	Next Action Prediction	Q: Following the conclusion of the 'calot triangle dissection' phase shown in the clip, what is the predicted key action that will begin the next phase? A: use clipper to clip blood vessel B: use hook to cut peritoneum C: use clipper to clip cystic duct D: use grasper to grasp liver	...the beginning use hook to dissect cystic artery, which indicates that the core dissection task of this phase has been completed...the key content of the next phase...clipping and cutting phase.	
	Next Phase Prediction	Q: Based on the surgical activity shown in this clip, which surgical phase immediately follows the 'calot triangle dissection' phase? A: gallbladder extraction phase B: gallbladder packaging phase C: clipping and cutting phase D: preparation phase	The current phase is the calot triangle dissection phase. From the captured video clip, we can observe at the beginning ... next phase will be the clipping and cutting phase.	
Counting	Object Counting	Q: How many distinct types of objects (e.g. tools, components, buttons as a single category) were visible in the video segment from 0.00s to 10.00s?? A: 10 B: 11 C: 12 D: 13	...battery, battery connector, board, electric screwdriver, oscilloscope...welder component, welder station. This amounts to a total of 11 distinct object types.	

Figure 12: Detailed examples of the 15 sub-tasks across our four core categories: Identification, Localization, Prediction, and Counting. For each sub-task, we present a representative question, the corresponding answer, and a visual frame from the video. These examples illustrate the diversity of our benchmark, spanning from low-level perception (e.g., object identification, spatial localization) to high-level reasoning (e.g., next action prediction, counting dynamic events).

1. Dominant Held-object Identification



Question: Which tool was the main surgeon left hand predominantly interacting with in the video segment from 0.00s to 10.00s?

- Options:**
A: hook
B: clipper
C: grasper
D: scissors

Detailed Answer: In the segment from 0.00s to 10.00s, the main surgeon left hand used: grasper: 10 times. 'grasper' was clearly the most frequent with 10 occurrences.

2. Object Not Visible Identification



Question: Which of the following objects was NOT visible in the video segment from 0.0s to 18s?

- Options:**
A: Skewer
B: Raspatory
C: Mouth Gag
D: Bipolar Forceps

Detailed Answer: In the video segment from 0.0s to 18s, the following (refined) object types were observed: [Bipolar Forceps, Mouth Gag, Raspatory, Suction Cannula]. Considering the options, 'Skewer' was not observed in this segment.

3. Object Spatial Localization



Question: Approximately in which region of the view was the 'grasper' (operated by main surgeon left hand) located around timestamp 3.33s?

- Options:**
A: top-right
B: top-left
C: top-center
D: center-right

Detailed Answer: Around 3.33s, the visible surgical instruments in the frame include: grasper, scissors. The 'grasper' operated by main surgeon left hand has a bounding box at coordinates [x=0.041, y=0.000, width=0.281, height=0.256] (normalized coordinates). Based on the tool's center point, it is located in the 'top-left' region of the 3x3 grid overlay (top-left, top-center, top-right, center-left, center, center-right, bottom-left, bottom-center, bottom-right).

4. Action Temporal Localization



Question: In this video segment, approximately at what timestamp does the assistant surgeon right hand first start grasp specimen bag using grasper?

- Options:**
A: 5.7s
B: 3.1s
C: 11.3s
D: 18.6s

Detailed Answer: In this video segment, 3 types of operators appeared: main surgeon left hand (MSLH), assistant surgeon right hand (ASRH), main surgeon right hand (MSRH)...The MSRHH performed use grasper to grasp specimen bag from 3.1s to 5.1s; performed use irrigator to retract liver from 5.1s to 9.1s; performed use irrigator to retract liver from 10.1s to 18.1s. The assistant surgeon right hand first started to grasp specimen bag using grasper at 2.1s and continued until 18.1s.

5. Next Phase Prediction



Question: Based on the surgical activity shown in this clip, which surgical phase immediately follows the 'clipping and cutting' phase?

- Options:**
A: gallbladder extraction phase
B: cleaning and coagulation phase
C: gallbladder packaging phase
D: gallbladder dissection phase

Detailed Answer: The current phase is the clipping and cutting phase. From the captured video clip, we can observe at the beginning use scissors to cut cystic duct, which indicates that the gallbladder's "lifeline" has been severed; while at the end of the clip, we can see use hook to dissect gallbladder, which is the key content of the next phase, we can predict that the next phase will be the gallbladder dissection phase.

6. Next Action Prediction



Question: Following the conclusion of the 'cleaning and coagulation' phase shown in the clip, what is the predicted key action that will begin the next phase?

- Options:**
A: use grasper to retract liver
B: use grasper to grasp specimen bag
C: use bipolar to dissect cystic plate
D: use irrigator to retract omentum

Detailed Answer: The current phase is the cleaning and coagulation phase. From the captured video clip, we can observe at the beginning use irrigator to aspirate fluid, which indicates that surgical field cleaning and final hemostasis have been completed; while at the end of the clip, we can see use grasper to grasp specimen bag, which is the key content of the next phase, we can predict that the next phase will be the gallbladder extraction phase.

7. Object Counting



Question: How many distinct types of surgical instruments were fully or partially visible in the video segment from 0.00s to 10.00s?

- Options:**
A: 4
B: 0
C: 1
D: 2

Detailed Answer: In the segment from 0.00s to 10.00s, the distinct instruments that were fully or partially visible include: grasper, hook. Total count: 2 distinct types of surgical instruments.

Figure 13: Representative QA examples from the Surgery domain.

1. Object Not Visible Identification



Question: Which of the following objects (using refined categories like 'button' for all buttons) was NOT visible in the video segment from 0.00s to 10.00s?

- Options:
A: battery
B: battery connector
C: board
D: oscilloscope

Detailed Answer: In the video segment from 0.00s to 10.00s, the following (refined) object types were observed: [battery, board, oscilloscope, screwdriver, socket, welder component, welder station]. Considering the options, 'battery connector' was not observed in this segment.

2. Dominant Held-object Identification



Question: Which tool was the operator's left hand predominantly interacting with in the video segment from 0.00s to 30.00s?

- Options:
A: battery
B: battery connector
C: board
D: button

Detailed Answer: During the segment from 0.00s to 30.00s, the operator's left hand had the following interaction dynamics: 'battery': 1 instance(s)... 'board': 3 instance(s), observed in 3 labelled frames. The tool 'board' was interacted with most frequently and/or for the longest based on timestamp analysis.

3. Object Spatial Localization



Question: Approximately in which region of the view was the electric screwdriver located when the operator's right hand was in contact with it around timestamp 2.37s (within segment 0.00s-10.00s)?

- Options:
A: bottom-center
B: bottom-left
C: bottom-right
D: center

Detailed Answer: An instance of interaction (contact) between the operator's right hand and the electric screwdriver was noted around 2.37s. At this moment, the electric screwdriver was determined to be in the 'center' region of the view. This is one example within the segment 0.00s to 10.00s.

4. Action Temporal Localization



Question: At what approximate timestamp did the operator's right hand perform the second 'contact' with the button within the video segment from 0.00s to 15.00s?

- Options:
A: 1.50s
B: 12.50s
C: 2.27s
D: 7.50s

Detailed Answer: Within the segment from 0.00s to 15.00s, the operator's right hand performed 'contact' with the button multiple times: the first at 1.20s, the second at 2.27s. The second occurrence was at approximately 2.27s.

5. Next Interaction Prediction



Question: Based on the activity observed up to 30.00s, what is the predicted next type of interaction for the operator's left hand?

- Options:
A: contact the board
B: contact the oscilloscope
C: contact the oscilloscope component
D: contact the screen

Detailed Answer: Observations up to 30.00s suggest a forthcoming interaction. During the observed context: at 2.93s, the right hand performed 'contact' with 'screen'...'screen' was visible in the context for approximately 1.00s...

6. Object Counting



Question: How many distinct types of objects (e.g. tools, components, buttons as a single category) were visible in the video segment from 0.00s to 10.00s?

- Options:
A: 10
B: 11
C: 12
D: 13

Detailed Answer: The special action 'jump' is performed in the video segment from 4s to 6s, demonstrating a distinctive athletic maneuver.

Figure 14: Representative QA examples from the Industry domain.

1. Special Action Identification



Question: What action is being performed in the video segment from 4s to 6s?

Options:

- A: Climb
- B: Spin
- C: Jump
- D: Fly

Detailed Answer: The special action 'jump' is performed in the video segment from 4s to 6s, demonstrating a distinctive athletic maneuver.

2. Sport Identification



Question: What extreme sport is being performed in the video segment?

Options:

- A: Mountain Bike
- B: Jetski
- C: Skiing
- D: Parkour

Detailed Answer: The video shows jetski activity based on the movement patterns and environment.

3. Action Sequence Identification



Question: What sequence of actions is performed in the time segment from 0s to 29s?

Options:

- A: Curveleft → Jump → Curveleft
- B: Leftright → Vault → Left
- C: Right → Flip → Left
- D: Right → Fly → Left

Detailed Answer: During the time segment from 0s to 29s, the performer executes the following sequence: Curveleft → Jump → Curveleft.

4. Action Temporal Localization



Question: At what approximate time does the 'walk' action begin in this video segment?

Options:

- A: 13.3s
- B: 6.7s
- C: 10.2s
- D: 2.3s

Detailed Answer: The 'walk' action begins at 10.2s in this video segment.

5. Next Direction Prediction



Question: Based on the video segment, what is the next direction of movement?

Options:

- A: Forward
- B: Left
- C: Left then right
- D: Curve right

Detailed Answer: Based on the movement patterns in the video segment, the next direction of movement is 'Forward'. The clip includes the following actions: right (3s-4s), left (4s-5s), right (5s-6s), curveleft (6s-11s), left (11s-15s).

Figure 15: Representative QA examples from the Extreme Sports domain.

1. Animal Identification



Question: What type of animal is featured in this egocentric video segment?

Options:

- A: Alligator
- B: Cheetah
- C: Turtle
- D: Lizard

Detailed Answer: The video shows a alligator from an egocentric perspective.

2. Interaction Identification



Question: What object is the dog interacting with in this video segment?

Options:

- A: Ball
- B: Person
- C: Bench
- D: Bird

Detailed Answer: The dog is interacting with a bench.

3. Interaction Temporal Localization



Question: When does the dog first interact with the person in this video clip?

Options:

- A: 9.0-13.0 seconds
- B: 2.5-6.5 seconds
- C: 30.8-34.8 seconds
- D: 66.2-70.2 seconds

Detailed Answer: The dog first interacts with the person from 7.0 to 15.0 seconds in this video clip.

Figure 16: Representative QA examples from the Animal Perspective domain.